



Original article

Design and synthesis of novel triazole antifungal derivatives by structure-based bioisosterism

Chunquan Sheng¹, Xiaoying Che¹, Wenya Wang, Shengzheng Wang, Yongbing Cao, Zhenyuan Miao, Jianzhong Yao*, Wannian Zhang**

School of Pharmacy, Second Military Medical University, 325 Guohe Road, Shanghai 200433, People's Republic of China

ARTICLE INFO

Article history:

Received 11 November 2010

Received in revised form

14 February 2011

Accepted 10 March 2011

Available online 17 March 2011

Keywords:

Structure-based bioisosterism

Triazolone

Azole

Antifungal

ABSTRACT

The incidence of life-threatening fungal infections is increasing dramatically. In an attempt to develop novel antifungal agents, our previously synthesized phenoxyalkylpiperazine triazole derivatives were used as lead structures for further optimization. By means of structure-based bioisosterism, triazolone was used as a new bioisostere of oxygen atom. This type of bioisosteric replacement can improve the water solubility without loss of hydrogen-bonding interaction with the target enzyme. A series of triazolone-containing triazoles were rationally designed and synthesized. As compared with fluconazole, several compounds showed higher antifungal activity with broader spectrum, suggesting their potential for further evaluations.

© 2011 Elsevier Masson SAS. All rights reserved.

1. Introduction

Over the past two decades, the incidence of systemic mycoses and associated mortality has increased dramatically [1,2]. This is primarily due to the increase in the number of immunocompromised individuals, such as patients receiving cancer chemotherapy or organ transplantation, and patients infected with human immunodeficiency virus. The most common fungal pathogens are species of *Candida*, *Cryptococcus* and *Aspergillus*. Clinically, amphotericin B (AmB) [3], triazoles (e.g. fluconazole and itraconazole, see Fig. 1) [4] and candins (e.g. caspofungin and micafungin) [5] are available to treat invasive fungal infections. However, these drugs were limited by their spectrum of activity, the development of resistance, non-optimal tolerability and drug–drug interactions. Therefore, there is an emergent need to develop novel antifungal agents with improved profiles.

Triazoles are the most widely used antifungal agents because of their high therapeutic index. They act by competitive inhibition of the lanosterol 14 α -demethylase (CYP51), a key enzyme in sterol biosynthesis of fungi [6]. To overcome the drawbacks of clinically available triazoles, numerous medicinal chemistry efforts have been

made to design and synthesize novel antifungal azoles. In order to improve the efficiency of azole optimization, we constructed three-dimensional (3D) models of fungal CYP51s by homology modeling [7–10]. Moreover, the CYP51-azole interactions were investigated by molecular docking [8,11]. On the basis of the results from molecular modeling, our group has designed highly potent azole derivatives with different C3-side chains [9,11–15]. Among them, azoles shown in Fig. 2 exhibited excellent *in vitro* activity with broad spectrum, representing promising leads for novel antifungal drug development [12]. Herein, triazolone was used as a new bioisostere of the side-chain oxygen atom in the lead structure. As a result, a series of potent antifungal triazoles were rationally designed and synthesized.

2. Chemistry

The oxirane intermediate **4** was synthesized by our previously reported procedure (Scheme 1) [11]. The triazolone-containing side chains **10a–t** were synthesized via six steps. In the presence of pyridine at ice bath, various substituted anilines **5a–t** were converted to phenylcarbamates **6a–t** by reacting with phenyl chloroformate. Phenylcarbamates **6a–t** was treated with hydrazine hydrate to give semicarbazide **7a–t**, which was subsequently reacted with formamidine acetate in the presence of DMF at 80 °C to give the triazolones **8a–t**. In the presence of K₂CO₃, compounds **8a–t** were treated with excess 1,3-dibromopropane in DMF at 65 °C

* Corresponding author. Tel./fax: +86 21 81871235.

** Corresponding author. Tel./fax: +86 21 81870243.

E-mail addresses: yaojz@sh163.net (J. Yao), zhangwnk@hotmail.com (W. Zhang).¹ These two authors contributed equally to this work.

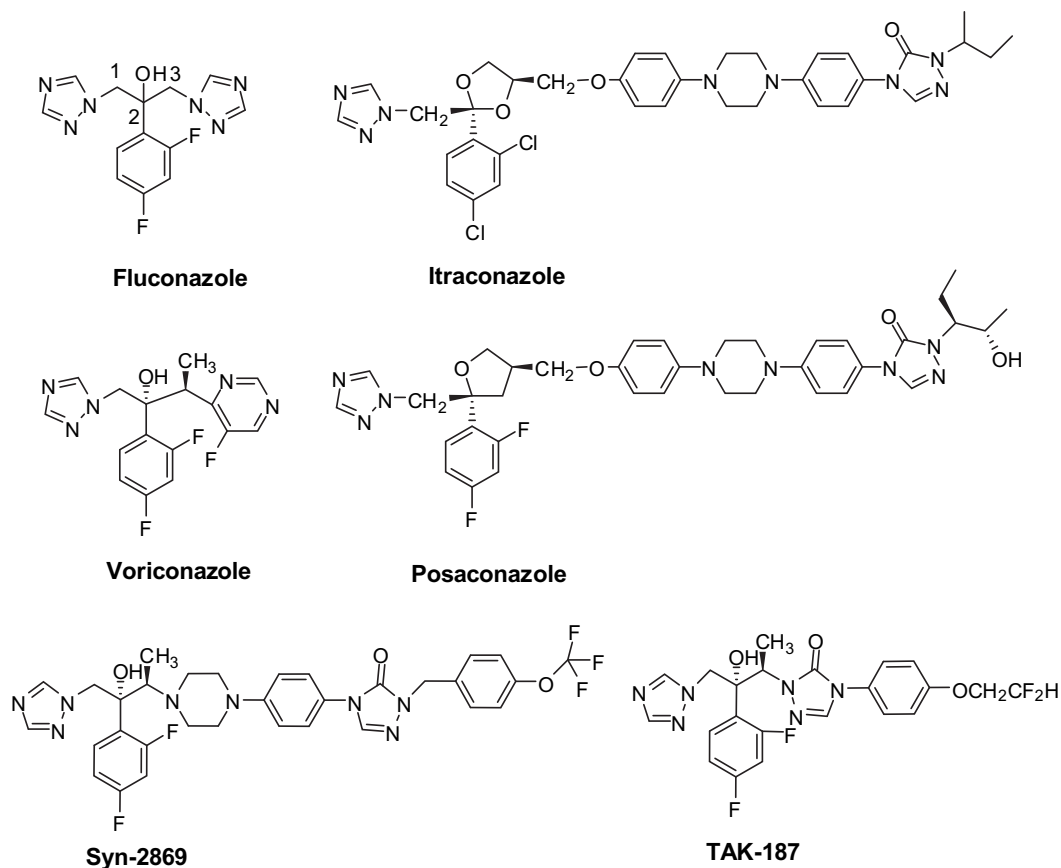


Fig. 1. Chemical structures of marketed and emerging triazole antifungal agents.

to afford compounds **9a–t**. Piperazine was substituted by **9a–t** using K_2CO_3 as base to yield triazolone side chains **10a–t**. The target compounds **11a–t** were obtained as racemates by a similar condition to our reported methods [12].

3. Microbiology

In vitro antifungal activity was measured according to the National Committee for Clinical Laboratory Standards (NCCLS) recommendations. The minimum inhibitory concentration (MIC) determination was performed by means of the serial dilution method in 96-well microtest plates with RPMI 1640 (Sigma) buffered with 0.165 M MOPS (Sigma) as the test medium. Fluconazole was used as the reference drug. Tested fungal strains were obtained from the ATCC or were clinical isolates. The MIC value was defined as the lowest concentration of test compounds that resulted in a culture with turbidity less than or equal to 80% inhibition when compared to the growth of the control. Test compounds were dissolved in DMSO serially diluted in growth medium. The yeasts were

incubated at 35 °C, and the growth MIC was determined at 24 h for *Candida* species, at 72 h for *Cryptococcus neoformans*, and at 7 days for filamentous fungi.

4. Results and discussion

4.1. Design rationale: structure-based bioisosterism

In our previous studies, we reported a series of new azoles with phenoxyalkylpiperazine side chains (Fig. 2) [12]. Because these compounds showed good antifungal activity, they were selected as starting points for further structure–activity relationship (SAR) studies. Molecular docking studies revealed that the lead compounds could form good hydrophobic, *van der Waals* and hydrogen-bonding interactions with *Candida albicans* CYP51 (CACYP51) [12]. Our rationale was focused on modifying the side chain without loss of key interactions. In the present investigation, triazolone group was used as a new bioisostere of lead structures to afford target compounds **11a–t**. This type of bioisosteric

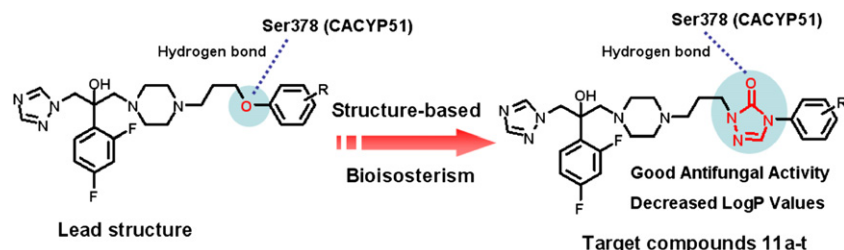
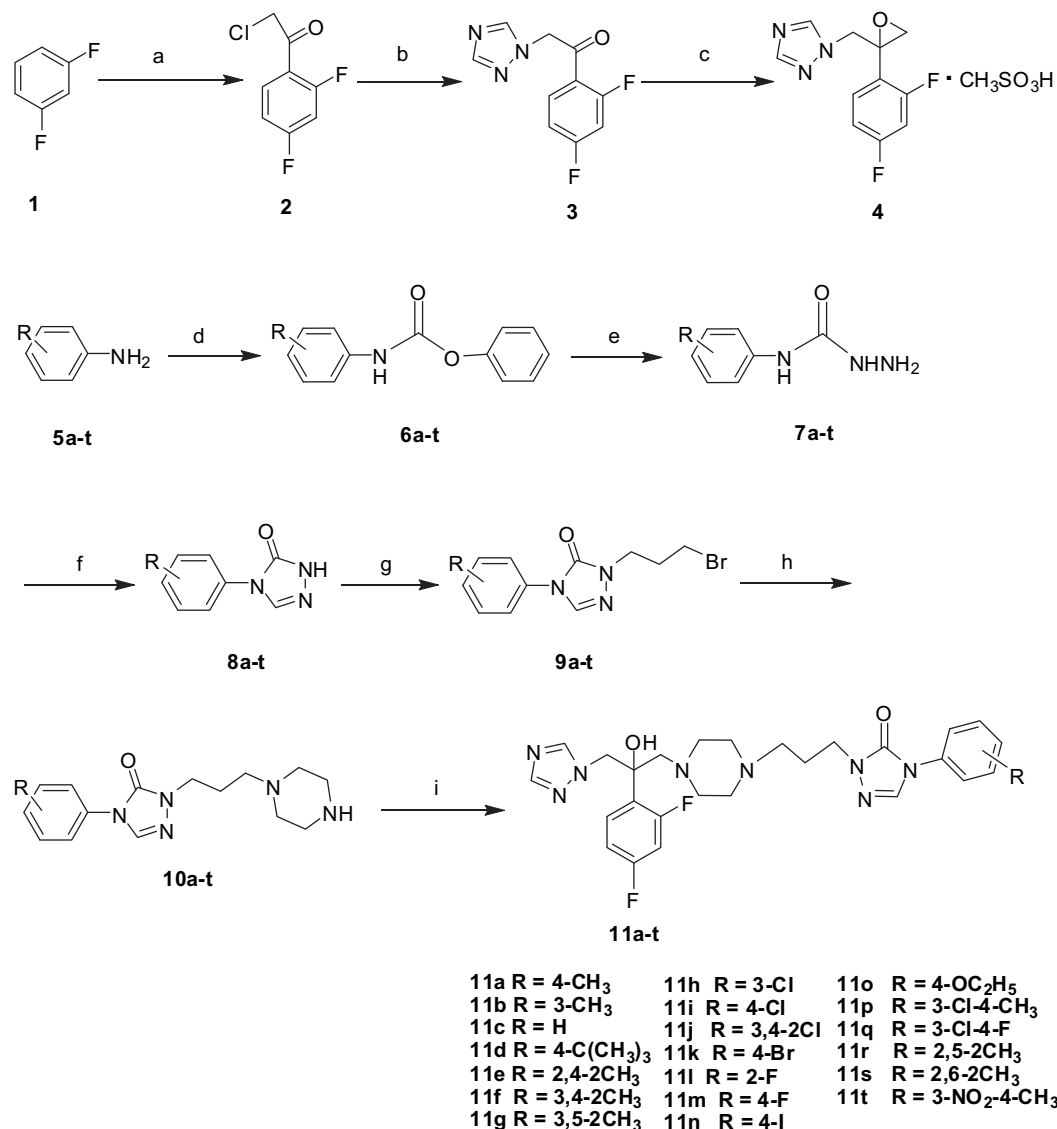


Fig. 2. Design rationale of the target compounds.



Scheme 1. Reagents and conditions: a. ClCH₂COCl, AlCl₃, CH₂Cl₂, 40 °C, 3 h, 50%; b. triazole, K₂CO₃, CH₂Cl₂, rt, 24 h, 70.0%; c. (CH₃)₃SOI, NaOH, toluene, 60 °C, 3 h, 62.3%; d. phenyl chloroformate, pyridine, acetoacetate, 0 °C ~ rt, 4 h, 69.9%–100%; e. 85% hydrazine hydrate, glycol dimethyl ether, rt, 24 h, 40.52%–83.01%; f. formamidine acetate, acetic acid, DMF, rt ~80 °C, 8 h, 39.38%–94.40%; g. 1,3-Dibromopropane, K₂CO₃, DMF, rt ~65 °C, 4.78%–16.15%; h. piperazine, K₂CO₃, EtOH, 70 °C, 8 h, 8.55%–75.0%; i. **4**, Et₃N, EtOH, reflux, 9 h, 18.3%–30.5%.

replacement was based on the following considerations: (1) Improve solubility and optimize pharmacokinetic profiles. Most of the marketed triazole antifungal agents have poor water solubility, leading to their low oral bioavailability. We compared the difference of LogP values between the target compounds and the lead structures by the method of Wang's group [16]. The non-classical bioisosteric replacement of the oxygen atom by the triazolone group led to decrease the LogP values by about 0.7 units. The LogP values of compounds **11a–t** are in the range of 1.92–3.59, suggesting their potential as oral active drugs. Moreover, the triazolone group seems to possess good drug-like properties because it can be found in many marketed or emerging triazole antifungal agents (such as itraconazole, posaconazole, TAK187, and Syn2869, see Fig. 1); (2) Keep the hydrogen-bonding interaction with Ser378. The carbonyl oxygen of the triazolone group can also function as a hydrogen bond acceptor able to interact with Ser378.

In order to validate the hypothesis, compound **11c** was docked into the active site of CACYP51 using the Affinity module within

InsightII 2000 software package [17], which has been proved to be a powerful tool to investigate azole-CYP51 interactions [11]. As shown in Fig. 3, compound **11c** shared a conformation similar to that of the lead structure in the active site [11,12]. The triazolone side chain was oriented into the S4 pocket [18] with its carbonyl oxygen atom forming a hydrogen bond with Ser378. Moreover, the piperazinyl moiety formed hydrophobic and *van der Waals* interactions with Leu376, Phe228 and Ile379, while the terminal phenyl group interacted with surrounding hydrophobic residues such as Phe85, Leu87, Met92 and Met508. The interaction energy between compound **11c** and CACYP51 was –79.3 kcal/mol, indicating that its affinity with CACYP51 was similar to that of the lead structure (interaction energy = –78.5 kcal/mol).

4.2. *In vitro* antifungal activities

In vitro antifungal activity of the synthesized compounds is reported in Table 1, which was expressed as the minimum

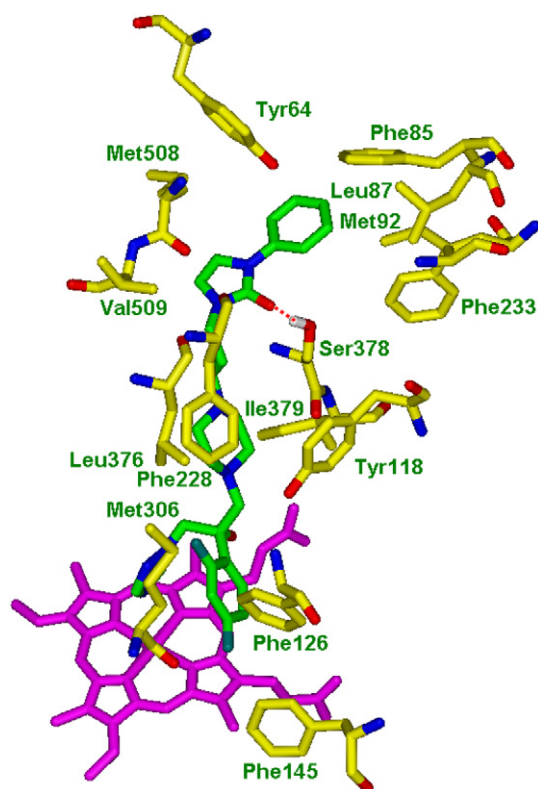


Fig. 3. The binding mode of compound 11c in the active site of CACYP51.

inhibitory concentration (MIC) that achieved 80% inhibition of the tested fungal pathogens using fluconazole as a reference drug. In general, most of the target compounds showed good inhibitory activity against the tested fungi, especially for *Candida* species.

Table 1
XlogP Value and *in vitro* antifungal activities of the target compounds (MIC₈₀, $\mu\text{g mL}^{-1}$).^a

Compd.	LogP	C. alb.	C. tro.	C. par.	C. kru.	C. neo.	A. fum.
11a	2.28	0.25	0.25	1	1	8	>64
11b	2.28	0.25	0.25	1	1	8	8
11c	1.92	0.25	1	1	1	8	>64
11d	3.59	0.25	0.25	0.25	0.25	1	1
11e	2.65	1	1	1	1	8	>64
11f	2.65	0.25	0.25	0.25	1	4	8
11g	2.65	0.25	0.25	1	1	4	8
11h	2.54	0.0625	0.0625	0.25	>64	4	16
11i	2.54	0.0625	0.25	0.25	0.25	4	8
11j	3.17	0.0625	0.0625	0.25	0.25	1	4
11k	2.61	0.25	0.25	0.25	1	4	8
11l	2.02	0.25	1	1	>64	>64	>64
11m	2.02	0.25	0.25	1	>64	>64	>64
11n	2.57	0.25	0.25	0.25	0.25	4	8
11o	2.25	0.25	1	1	1	8	>64
11p	2.91	0.0625	0.25	0.25	0.25	1	4
11q	2.65	0.0625	0.0625	0.25	0.25	1	4
11r	2.65	0.25	0.25	1	1	8	>64
11s	2.65	1	0.25	4	1	>64	>64
11t	2.11	0.25	0.25	1	>64	16	>64
FCZ	0.35	0.25	0.0625	1	0.25	16	>64

^a Abbreviations: *C. alb.*, *Candida albicans* (Strain number: Y0109); *C. tro.*, *Candida tropicalis* (Strain number: 087); *C. par.*, *Candida parapsilosis* (Strain number: ATCC 22019); *C. kru.*, *Candida krusei* (Strain number: ATCC 6258); *C. neo.*, *Cryptococcus neoformans* (Strain number: 32609); *A. Fum.*, *Aspergillus fumigatus* (Strain number: 7544); FLZ, Fluconazole.

Except compounds **11e** and **11s**, the MIC range for *C. albicans* was 0.25 $\mu\text{g/mL}$ to 0.0625 $\mu\text{g/mL}$, indicating that these compounds were comparable or superior to fluconazole. Good activity of them was also observed for *Candida tropicalis* (MIC range: 0.25 $\mu\text{g/mL}$ to 1 $\mu\text{g/mL}$), and compounds **11h**, **11j** and **11q** showed comparable activity to fluconazole. On the *Candida parapsilosis* strain, nine compounds (**11d**, **11f**, **11h**, **11i**, **11j**, **11k**, **11n**, **11p** and **11q**) were more active (MIC = 0.25 $\mu\text{g/mL}$) than fluconazole (MIC = 1 $\mu\text{g/mL}$). Most of the compounds showed decreased activity against *Candida krusei*. Compounds **11h**, **11l**, **11m** and **11t** were totally inactive, suggesting that the active site of CYP51 from *C. krusei* might have different properties. Most of the compounds including fluconazole only showed moderate activity against *C. neoformans*. Among them, compounds **11j**, **11p** and **11q** (MIC = 1 $\mu\text{g/mL}$) were 16 fold more potent than fluconazole (MIC = 16 $\mu\text{g/mL}$). Fluconazole is inactive against *Aspergillus fumigatus*, while several target compounds showed moderate to good activity (MIC range: 1 $\mu\text{g/mL}$ to 8 $\mu\text{g/mL}$). In particular, compound **11c** was the most active one with MIC value of 1 $\mu\text{g/mL}$. Serious drug resistance has been a major problem for the clinical application of azole antifungal agents. Two representative compounds, **11c** and **11i**, were tested their inhibitory activities against azole-resistant strain of *C. albicans*. The MIC value of for compounds **11c** and **11i** was 1 $\mu\text{g/mL}$ and 0.125 $\mu\text{g/mL}$, respectively. Because of their good activity toward azole-resistant clinical isolate, it is important to subject the highly active compounds (e.g. **11d**, **11i**, **11j**, **11p** and **11q**) for further evaluation.

4.3. Structure–activity relationships

From the antifungal activity data, preliminary SARs of the synthesized azoles were obtained. In general, the substitutions on the terminal phenyl group were important for the antifungal activities. As compared with compound **3c**, the introduction of a chlorine atom on position 4 of the terminal phenyl group (compound **11i**) led to the improvement of the antifungal activity and spectrum. For compounds with other substitutions on position 4 (i.e. F, Br, I, methyl, ethoxy and *tert*-butyl), they showed the same activity against *C. albicans* as the non-substituted derivative **11c**, but their antifungal spectrum was improved. For example, 4-*tert*-butyl derivative **11d** can also significantly inhibit the growth of *C. neoformans* and *A. fumigatus*. If the chlorine atom of compound **11i** was moved to position 3 (compound **11h**), good activity was retained. Moreover, several di-halogen substituted derivatives (e.g. **11j** and **11q**) showed improved antifungal activity and spectrum. On the other hand, dimethyl substitution on the phenyl group (compounds **11e**, **11f**, **11g**, **11r** and **11s**) had little effect on the antifungal activity. For 4-methyl derivative **11a**, the addition of a chlorine atom on position 3 (compound **11p**) led to the increase of the antifungal activity, while adding a nitro group on position 3 did not show positive effect. From the above analysis, 4-chlorine and 3,4-dihalogen substitutions were found to be the most favorable for the antifungal activity and spectrum.

Moreover, it was observed that the LogP values of the compounds correlated well with their antifungal activities. This trend was particularly obvious for the inhibitory activities against *A. fumigatus*. Generally, more hydrophobic compounds were more active toward *A. fumigatus*. For example, the most hydrophobic compounds **11d**, **11j** and **11p** showed the best anti-*A. fumigatus* activities, whereas the compounds with lowest LogP values (e.g. **11a**, **11l**, **11m** and **11t**) were totally inactive. It is also worth noting that all the synthesized compounds are racemates and the isomers might have different antifungal activities. On the basis of our previous studies, the *R* isomers showed lower interaction energy with CACYP51 than the *S* isomers [11], suggesting that the *R* isomers

might have better antifungal activity. In our next studies, we will focus on synthesizing optically pure isomers and comparing their antifungal activities.

5. Conclusion

Bioisosterism is a very useful drug design method to improve pharmacological activity, gain selectivity and optimize the pharmacokinetics of the lead compounds [19,20]. In the present investigation, we provide an example of using triazolone as a new bioisotere of oxygen atom. Molecular modeling studies indicated this type of bioisosterism had several advantages such as improvement of the water solubility, and preservation of key hydrogen-bonding interaction with the receptor. The designed new triazole derivatives have good antifungal activity toward a wide range of pathogenic fungi including clinical resistant isolate, suggesting that structure-based bioisosterism might be developed into a useful approach in lead optimization. Because of the lack of CACYP51 inhibitory activity data, the present type of non-classical bioisosterism remains to be further investigated.

6. Experimental protocols

6.1. General procedure for the synthesis of compounds

Nuclear magnetic resonance (NMR) spectra were recorded on a Bruker 500 spectrometer with TMS as an internal standard and CDCl₃ as solvent. Chemical shifts (δ values) and coupling constants (J values) are given in ppm and Hz, respectively. ESI mass spectra were performed on an API-3000 LC–MS spectrometer. High-resolution mass spectrometry measurements were performed on a Kratos-concep mass spectrometer under electron impact ionization (EI) conditions. Elemental analyses were performed with a MOD-1106 instrument and are consistent with theoretical values within $\pm 0.4\%$. TLC analysis was carried out on silica gel plates GF254 (Qingdao Haiyang Chemical, China). Silica gel column chromatography was performed with Silica gel 60G (Qingdao Haiyang Chemical, China). Commercial solvents were used without any pretreatment.

6.1.1. Phenyl *p*-tolylcarbamate (**6a**)

Phenyl chloroformate (17.2 g, 0.11 mol) was added dropwise to a stirred mixture of *p*-toluidine (23.6 g, 0.1 mol), pyridine (8.5 g, 0.11 mol) and EtOAc (200 mL) at 0 °C. The mixture was stirred for 3 h at room temperature, then washed with water (200 mL \times 3), dried over anhydrous Na₂SO₄, and filtrated. The solvent was evaporated under reduced pressure and the deposited solid were collected and washed with hexane to give **6a** as yellow solid (19.71 g, 92.5%). The product can be used directly in the next step without further purification. ¹H NMR (500 MHz, CDCl₃, TMS): δ 10.11 (s, 1H), 6.74–7.44 (m, 9H), 2.55 (s, 3H). MS (ESI) m/z : 228 (M + 1). The synthetic procedure for compounds **6b–t** was similar to the synthesis of compound **6a**.

6.1.2. *N*-*p*-Tolylhydrazinecarboxamide (**7a**)

A mixture of compound **6a** (19.19 g, 0.09 mol), 85% hydrazine hydrate (9 mL) and dimethoxyethane (135 mL) was stirred for 24 h. The solvent was evaporated under reduced pressure and the residue was washed with EtOAc to give **7a** as white solid (8.24 g, 60.59%). The product can be used directly in the next step without further purification. ¹H NMR (500 MHz, CDCl₃, TMS): δ 8.03 (br, 1H), 7.10–7.35 (m, 4H), 6.07 (br, 1H), 3.82 (br, 2H), 2.30 (s, 3H). MS (ESI) m/z : 166 (M + 1). The synthetic procedure for compounds **7b–t** was similar to the synthesis of compound **7a**.

6.1.3. 4-*p*-Tolyl-1*H*-1,2,4-triazol-5(4*H*)-one (**8a**)

A mixture of compound **7a** (7.56 g, 0.05 mol), formamidine acetate (22.0 g, 0.2 mol) and DMF (250 mL) was stirred at room temperature for 30 min. AcOH (15 mL) was added, and the resulting mixture was heated for 8 h at 80 °C. The solvent was evaporated under reduced pressure and the residue was poured into the ice water. After filtration, the residue was recrystallized from EtOAc–hexane to give **8a** as pale yellow solid (4.25 g, 52.73%). The product can be used directly in the next step without further purification. ¹H NMR (500 MHz, CDCl₃, TMS): δ 10.38 (br, 1H), 7.67 (s, 1H), 7.26–7.42 (m, 4H), 2.40 (s, 1H). MS (ESI) m/z : 174 (M + 1). The synthetic procedure for compounds **8b–t** was similar to the synthesis of compound **8a**.

6.1.4. 1-(3-Bromopropyl)-4-*p*-tolyl-1*H*-1,2,4-triazol-5(4*H*)-one (**9a**)

A solution of compound **8a** (0.32 g, 0.002 mol) in DMF (5 mL) was added dropwise to the suspension of 1,3-dibromopropane (0.61 g, 0.003 mol), K₂CO₃ (0.55 g, 0.004 mol) and DMF (10 mL). The resulting mixture was stirred at 65 °C for 10 h, then diluted with H₂O (50 mL) and extracted with ethyl acetate (20 mL \times 3). The combined organic layers were washed with H₂O (50 mL \times 3), dried over anhydrous Na₂SO₄, and filtrated, and the solvent was evaporated under reduced pressure. The residue was purified by silica gel column chromatography (hexane: EtOAc = 5:1, v/v) to give **9a** as pale yellow solid (0.25 g, yield 39.93%). ¹H NMR (500 MHz, CDCl₃, TMS): δ 7.06 (s, 1H), 7.26–7.42 (m, 4H), 4.02 (t, J = 6.6 Hz, 2H), 3.49 (t, J = 6.6 Hz, 2H), 2.38 (s, 3H), 2.36 (2H, m). MS (ESI) m/z : 313 (M + 1). The synthetic procedure for compounds **9b–t** was similar to the synthesis of compound **9a**.

6.1.5. 1-(3-(Piperazin-1-yl)propyl)-4-*p*-tolyl-1*H*-1,2,4-triazol-5(4*H*)-one (**10a**)

A solution of compound **9a** (0.24 g, 0.85 mmol) in ethanol (5 mL) was added dropwise to the suspension of anhydrous piperazine (0.08 g, 0.94 mmol), K₂CO₃ (0.18 g, 1.28 mmol) and ethanol (10 mL). The resulting mixture was stirred at reflux for 8 h, then evaporated under reduced pressure. The residue was purified by silica gel column chromatography (CH₂Cl₂:CH₃OH = 10:1, v/v) to give **10a** as pale yellow solid (0.09 g, yield 37.5%). ¹H NMR (500 MHz, CDCl₃, TMS): δ 7.64 (s, 1H), 7.26–7.41 (m, 4H), 3.92 (t, J = 6.7 Hz, 2H), 3.13 (br, 4H), 2.69 (br, 4H), 2.52 (t, J = 6.7 Hz, 2H), 2.38 (s, 3H), 1.95 (m, 2H). The synthetic procedure for compounds **10b–t** was similar to the synthesis of compound **10a**.

6.1.6. 1-(3-(4-(2-(2,4-Difluorophenyl)-2-hydroxy-3-(1*H*-1,2,4-triazol-1-yl)propyl) piperazin-1-yl)propyl)-4-(4-methylphenyl)-1*H*-1,2,4-triazol-5(4*H*)-one (**11a**)

A solution of epoxide **4** (0.13 g, 0.4 mmol), **10a** (0.094 g, 0.3 mmol), triethylamine (1 mL) and EtOH (10 mL) were heated to reflux for 8 h. The solvent was evaporated under reduced pressure. The residue was purified by silica gel column chromatography (CH₂Cl₂:MeOH 100:2, v/v) to give **11a** as pale yellow oil (0.07 g, yield 44.48%). ¹H NMR (500 MHz, CDCl₃, TMS): δ 8.11 (s, 1H), 7.78 (s, 1H), 7.65 (s, 1H), 6.77–7.62 (m, 7H), 5.30 (s, 1H), 4.52 (s, 2H), 3.88 (t, J = 6.7 Hz, 2H), 3.05 (d, J = 13.4 Hz, 1H), 2.67 (d, J = 10.8 Hz, 1H), 2.39 (br, 10H), 2.38 (s, 3H), 2.02 (m, 2H). MS (ESI) m/z : 539 (M + 1). Anal. calcd for C₂₇H₃₂F₂N₈O₂: C 60.21, H 5.99, N 20.80, found: C 60.33, H 5.97, N 20.76.

6.1.7. 1-(3-(4-(2-(2,4-Difluorophenyl)-2-hydroxy-3-(1*H*-1,2,4-triazol-1-yl)propyl) piperazin-1-yl)propyl)-4-(3-methylphenyl)-1*H*-1,2,4-triazol-5(4*H*)-one (**11b**)

¹H NMR (500 MHz, CDCl₃, TMS): δ 8.14 (s, 1H), 7.78 (s, 1H), 7.64 (s, 1H), 6.78–7.53 (m, 7H), 5.30 (s, 1H), 4.50 (dd, 2H, J_1 = 3.3 Hz, J_2 = 14.4 Hz), 3.87 (m, 2H), 3.04 (d, 1H, J = 13.8 Hz), 2.64 (d, 1H,

$J = 13.6$ Hz), 2.38 (s, 3H), 2.34 (br, 10H), 1.90 (m, 2H). MS (ESI) m/z : 538 (M). Anal. calcd for $C_{27}H_{32}F_2N_8O_2$: C 60.21, H 5.99, N 20.80, found: C 60.39, H 5.97, N 20.72.

6.1.8. 1-(3-(4-(2-(2,4-Difluorophenyl)-2-hydroxy-3-(1H-1,2,4-triazol-1-yl)propyl) piperazin-1-yl)propyl)-4-phenyl-1H-1,2,4-triazol-5(4H)-one (**11c**)

1H NMR (500 MHz, $CDCl_3$, TMS): δ 8.13 (s, 1H), 7.79 (s, 1H), 7.67 (s, 1H), 6.79–7.54 (m, 8H), 5.30 (s, 1H), 4.50 (d, $J = 2.4$ Hz, 2H), 3.88 (t, $J = 6.9$ Hz, 2H), 3.04 (d, $J = 13.8$ Hz, 1H), 2.64 (d, $J = 13.6$ Hz, 1H), 2.37 (br, 10H), 1.90 (m, 2H). ^{13}C NMR (500 MHz, $CDCl_3$, TMS): δ 163.63, 161.59, 159.84, 157.87, 151.70, 150.92, 144.53, 133.84, 133.44, 129.54, 129.24, 127.48, 126.08, 111.44, 104.18, 71.95, 62.18, 56.28, 55.09, 54.03, 53.34, 52.91, 43.76, 25.56. MS (ESI) m/z : 525 (M + 1). Anal. calcd for $C_{26}H_{30}F_2N_8O_2$: C 59.53, H 5.76, N 21.36, found: C 59.64, H 5.73, N 21.33.

6.1.9. 1-(3-(4-(2-(2,4-Difluorophenyl)-2-hydroxy-3-(1H-1,2,4-triazol-1-yl)propyl) piperazin-1-yl)propyl)-4-(4-tert-butylphenyl)-1H-1,2,4-triazol-5(4H)-one (**11d**)

1H NMR (300 MHz, $CDCl_3$, TMS): δ 8.14 (s, 1H), 7.78 (s, 1H), 7.63 (s, 1H), 6.77–7.54 (m, 7H), 5.31 (s, 1H), 4.51 (s, 2H), 3.87 (t, $J = 6.9$ Hz, 2H), 3.05 (d, $J = 13.5$ Hz, 1H), 2.64 (d, $J = 13.5$ Hz, 1H), 2.38 (br, 10H), 1.91 (m, 2H), 1.34 (s, 9H). MS (ESI) m/z : 581 (M + 1). Anal. calcd for $C_{30}H_{38}F_2N_8O_2$: C 62.05, H 6.60, N 19.30, found: C 61.92, H 6.61, N 19.37.

6.1.10. 1-(3-(4-(2-(2,4-Difluorophenyl)-2-hydroxy-3-(1H-1,2,4-triazol-1-yl)propyl) piperazin-1-yl)propyl)-4-(2,4-dimethylphenyl)-1H-1,2,4-triazol-5(4H)-one (**11e**)

1H NMR (500 MHz, $CDCl_3$, TMS): δ 8.13 (s, 1H), 7.78 (s, 1H), 7.39 (s, 1H), 6.78–7.56 (m, 6H), 5.30 (s, 1H), 4.51 (d, $J = 2.3$ Hz, 2H), 3.86 (t, $J = 7.0$ Hz, 2H), 3.06 (d, $J = 13.4$ Hz, 1H), 2.66 (d, $J = 13.5$ Hz, 1H), 2.46 (br, 10H), 2.35 (s, 3H), 2.26 (s, 3H), 1.94 (m, 2H). MS (ESI) m/z : 552 (M). Anal. calcd for $C_{28}H_{34}F_2N_8O_2$: C 60.86, H 6.20, N 20.28, found: C 60.62, H 6.19, N 20.34.

6.1.11. 1-(3-(4-(2-(2,4-Difluorophenyl)-2-hydroxy-3-(1H-1,2,4-triazol-1-yl)propyl) piperazin-1-yl)propyl)-4-(3,4-dimethylphenyl)-1H-1,2,4-triazol-5(4H)-one (**11f**)

1H NMR (500 MHz, $CDCl_3$, TMS): δ 8.14 (s, 1H), 7.78 (s, 1H), 7.60 (s, 1H), 6.78–7.56 (m, 6H), 5.30 (s, 1H), 4.50 (dd, $J_1 = 3.0$ Hz, $J_2 = 14.3$ Hz, 2H), 3.86 (t, $J = 7.0$ Hz, 2H), 3.04 (d, $J = 13.6$ Hz, 1H), 2.64 (d, $J = 13.6$ Hz, 1H), 2.37 (br, 10H), 2.30 (s, 3H), 2.28 (s, 3H), 1.91 (m, 2H). MS (ESI) m/z : 552 (M). Anal. calcd for $C_{28}H_{34}F_2N_8O_2$: C 60.86, H 6.20, N 20.28, found: C 60.73, H 6.22, N 20.30.

6.1.12. 1-(3-(4-(2-(2,4-Difluorophenyl)-2-hydroxy-3-(1H-1,2,4-triazol-1-yl)propyl) piperazin-1-yl)propyl)-4-(3,5-dimethylphenyl)-1H-1,2,4-triazol-5(4H)-one (**11g**)

1H NMR (500 MHz, $CDCl_3$, TMS): δ 8.12 (s, 1H), 7.78 (s, 1H), 7.62 (s, 1H), 6.77–7.55 (m, 6H), 4.52 (dd, $J_1 = 3.0$ Hz, $J_2 = 14.3$ Hz, 2H), 3.87 (t, $J = 6.85$ Hz, 2H), 3.05 (d, $J = 13.4$ Hz, 1H), 2.65 (d, $J = 13.5$ Hz, 1H), 2.39 (br, 10H), 2.35 (s, 6H, CH_3), 1.95 (m, 2H). MS (ESI) m/z : 552 (M). Anal. calcd for $C_{28}H_{34}F_2N_8O_2$: C 60.86, H 6.20, N 20.28, found: C 60.68, H 6.21, N 20.32.

6.1.13. 1-(3-(4-(2-(2,4-Difluorophenyl)-2-hydroxy-3-(1H-1,2,4-triazol-1-yl)propyl) piperazin-1-yl)propyl)-4-(3-chlorophenyl)-1H-1,2,4-triazol-5(4H)-one (**11h**)

1H NMR (500 MHz, $CDCl_3$, TMS): δ 8.14 (s, 1H), 7.78 (s, 1H), 7.66 (s, 1H), 6.79–7.62 (m, 7H), 5.30 (s, 1H), 4.50 (d, $J = 3.69$ Hz, 2H), 3.87 (t, $J = 7.0$ Hz, 2H), 3.04 (d, $J = 13.5$ Hz, 1H), 2.64 (d, $J = 13.6$ Hz, 1H), 2.34 (br, 10H), 1.91 (m, 2H). Anal. calcd for $C_{26}H_{29}ClF_2N_8O_2$: C 55.86, H 5.23, N 20.04, found: C 55.92, H 5.21, N 20.00.

6.1.14. 1-(3-(4-(2-(2,4-Difluorophenyl)-2-hydroxy-3-(1H-1,2,4-triazol-1-yl)propyl) piperazin-1-yl)propyl)-4-(4-chlorophenyl)-1H-1,2,4-triazol-5(4H)-one (**11i**)

1H NMR (500 MHz, $CDCl_3$, TMS): δ 8.14 (s, 1H), 7.78 (s, 1H), 7.65 (s, 1H), 6.79–7.54 (m, 7H), 5.30 (s, 1H), 4.50 (dd, $J_1 = 5.2$ Hz, $J_2 = 14.3$ Hz, 2H), 3.86 (t, $J = 6.9$ Hz, 2H), 3.04 (d, $J = 13.5$ Hz, 1H), 2.64 (d, $J = 13.5$ Hz, 1H), 2.34 (br, 10H), 1.91 (m, 2H). MS (ESI) m/z : 560 (M + 1). Anal. calcd for $C_{26}H_{29}ClF_2N_8O_2$: C 55.86, H 5.23, N 20.04, found: C 55.84, H 5.24, N 20.08.

6.1.15. 1-(3-(4-(2-(2,4-Difluorophenyl)-2-hydroxy-3-(1H-1,2,4-triazol-1-yl)propyl) piperazin-1-yl)propyl)-4-(3,4-dichlorophenyl)-1H-1,2,4-triazol-5(4H)-one (**11j**)

1H NMR (500 MHz, $CDCl_3$, TMS): δ 8.14 (s, 1H), 7.78 (s, 1H), 7.66 (s, 1H), 6.79–7.75 (m, 6H), 5.30 (s, 1H), 4.50 (dd, $J_1 = 5.8$ Hz, $J_2 = 14.3$ Hz, 2H), 3.86 (t, $J = 6.9$ Hz, 2H), 3.04 (d, $J = 13.8$ Hz, 1H), 2.64 (d, $J = 13.6$ Hz, 1H), 2.33 (br, 10H), 1.90 (m, 2H). MS (ESI) m/z : 594 (M + 1). Anal. calcd for $C_{26}H_{28}Cl_2F_2N_8O_2$: C 52.62, H 4.76, N 18.88, found: C 52.46, H 4.77, N 18.93.

6.1.16. 1-(3-(4-(2-(2,4-Difluorophenyl)-2-hydroxy-3-(1H-1,2,4-triazol-1-yl)propyl) piperazin-1-yl)propyl)-4-(4-bromophenyl)-1H-1,2,4-triazol-5(4H)-one (**11k**)

1H NMR (500 MHz, $CDCl_3$, TMS): δ 8.14 (s, 1H), 7.78 (s, 1H), 7.65 (s, 1H), 6.78–7.60 (m, 7H), 5.30 (s, 1H), 4.50 (dd, $J_1 = 5.0$ Hz, $J_2 = 15.0$ Hz, 2H), 3.86 (t, $J = 7.0$ Hz, 2H), 3.05 (d, $J = 13.4$ Hz, 1H), 2.65 (d, $J = 13.6$ Hz, 1H), 2.36 (br, 10H), 1.91 (m, 2H). MS (ESI) m/z : 604 (M + 1). Anal. calcd for $C_{26}H_{29}BrF_2N_8O_2$: C 51.75, H 4.84, N 18.57, found: C 51.72, H 4.85, N 18.59.

6.1.17. 1-(3-(4-(2-(2,4-Difluorophenyl)-2-hydroxy-3-(1H-1,2,4-triazol-1-yl)propyl) piperazin-1-yl)propyl)-4-(2-fluorophenyl)-1H-1,2,4-triazol-5(4H)-one (**11l**)

1H NMR (500 MHz, $CDCl_3$, TMS): δ 8.14 (s, 1H), 7.77 (s, 1H), 7.63 (s, 1H), 6.78–7.67 (m, 7H), 5.30 (s, 1H), 4.50 (dd, $J_1 = 2.0$ Hz, $J_2 = 14.4$ Hz, 2H), 3.86 (t, $J = 7.0$ Hz, 2H), 3.05 (d, $J = 13.6$ Hz, 1H), 2.64 (d, $J = 13.6$ Hz, 1H), 2.36 (br, 10H), 1.92 (m, 2H). Anal. calcd for $C_{26}H_{29}F_3N_8O_2$: C 57.56, H 5.39, N 20.65, found: C 57.68, H 5.37, N 20.61.

6.1.18. 1-(3-(4-(2-(2,4-Difluorophenyl)-2-hydroxy-3-(1H-1,2,4-triazol-1-yl)propyl) piperazin-1-yl)propyl)-4-(4-fluorophenyl)-1H-1,2,4-triazol-5(4H)-one (**11m**)

1H NMR (500 MHz, $CDCl_3$, TMS): δ 8.13 (s, 1H), 7.78 (s, 1H), 7.62 (s, 1H), 6.78–7.55 (m, 7H), 5.30 (s, 1H), 4.50 (dd, $J_1 = 3.8$ Hz, $J_2 = 14.6$ Hz, 2H), 3.86 (t, $J = 6.7$ Hz, 2H), 3.04 (d, $J = 13.6$ Hz, 1H), 2.65 (d, $J = 12.6$ Hz, 1H), 2.36 (br, 10H), 1.92 (m, 2H). Anal. calcd for $C_{26}H_{29}F_3N_8O_2$: C 57.56, H 5.39, N 20.65, found: C 57.64, H 5.36, N 20.62.

6.1.19. 1-(3-(4-(2-(2,4-Difluorophenyl)-2-hydroxy-3-(1H-1,2,4-triazol-1-yl)propyl) piperazin-1-yl)propyl)-4-(4-iodophenyl)-1H-1,2,4-triazol-5(4H)-one (**11n**)

1H NMR (500 MHz, $CDCl_3$, TMS): δ 8.10 (s, 1H), 7.81 (s, 1H), 7.80 (s, 1H), 6.79–7.80 (m, 7H), 5.30 (s, 1H), 4.50 (s, 2H), 3.89 (t, $J = 6.7$ Hz, 2H), 3.08 (d, $J = 13.6$ Hz, 1H), 2.71 (d, $J = 13.8$ Hz, 1H), 2.55 (br, 10H), 2.23 (m, 2H). MS (ESI) m/z : 651 (M + 1). Anal. calcd for $C_{26}H_{29}F_2IN_8O_2$: C 48.01, H 4.49, N 17.23, found: C 48.10, H 4.47, N 17.18.

6.1.20. 1-(3-(4-(2-(2,4-Difluorophenyl)-2-hydroxy-3-(1H-1,2,4-triazol-1-yl)propyl) piperazin-1-yl)propyl)-4-(4-ethoxyphenyl)-1H-1,2,4-triazol-5(4H)-one (**11o**)

1H NMR (500 MHz, $CDCl_3$, TMS): δ 8.13 (s, 1H), 7.78 (s, 1H), 7.58 (s, 1H), 6.78–7.75 (m, 7H), 5.30 (s, 1H), 4.50 (dd, $J_1 = 2.1$ Hz,

$J_2 = 14.4$ Hz, 2H), 4.05 (m, 2H), 3.86 (t, $J = 6.9$ Hz, 2H), 3.05 (d, $J = 12.4$ Hz, 1H), 2.65 (d, $J = 13.6$ Hz, 1H), 2.36 (br, 10H), 1.93 (m, 2H), 1.43 (t, $J = 7.0$ Hz, 3H). Anal. calcd for $C_{28}H_{34}F_2N_8O_3$: C 59.14, H 6.03, N 19.71, found: C 59.08, H 6.04, N 19.76.

6.1.21. 1-(3-(4-(2-(2,4-Difluorophenyl)-2-hydroxy-3-(1H-1,2,4-triazol-1-yl)propyl) piperazin-1-yl)propyl)-4-(3-chloro-4-methylphenyl)-1H-1,2,4-triazol-5(4H)-one (**11p**)

1H NMR (300 MHz, $CDCl_3$, TMS): δ 8.13 (s, 1H), 8.10 (s, 1H), 7.77 (s, 1H), 6.75–7.72 (m, 6H), 5.30 (br, 1H), 4.48 (dd, $J_1 = 7.5$ Hz, $J_2 = 15.0$ Hz, 2H), 3.86 (t, $J = 7.0$ Hz, 2H), 3.04 (d, $J = 13.5$ Hz, 1H), 2.65 (d, $J = 13.5$ Hz, 1H), 2.39 (s, 3H), 2.36 (br, 10H), 1.89 (m, 2H). MS (ESI) m/z : 574 ($M + 1$). Anal. calcd for $C_{27}H_{31}ClF_2N_8O_2$: C 56.59, H 5.45, N 19.55, found: C 56.70, H 5.43, N 19.48.

6.1.22. 1-(3-(4-(2-(2,4-Difluorophenyl)-2-hydroxy-3-(1H-1,2,4-triazol-1-yl)propyl) piperazin-1-yl)propyl)-4-(3-chloro-4-fluorophenyl)-1H-1,2,4-triazol-5(4H)-one (**11q**)

1H NMR (300 MHz, $CDCl_3$, TMS): δ 8.14 (s, 1H), 7.78 (s, 1H), 7.64 (s, 1H), 6.76–7.69 (m, 6H), 5.30 (s, 1H), 4.50 (dd, $J_1 = 7.5$ Hz, $J_2 = 15.0$ Hz, 2H), 3.86 (t, $J = 7.0$ Hz, 2H), 3.05 (d, $J = 13.5$ Hz, 1H), 2.64 (d, $J = 13.8$ Hz, 1H), 2.36 (br, 10H), 1.90 (m, 2H). MS (ESI) m/z : 578 ($M + 1$). Anal. calcd for $C_{26}H_{28}ClF_3N_8O_2$: C 54.12, H 4.89, N 19.42, found: C 54.02, H 4.88, N 19.47.

6.1.23. 1-(3-(4-(2-(2,4-Difluorophenyl)-2-hydroxy-3-(1H-1,2,4-triazol-1-yl)propyl) piperazin-1-yl)propyl)-4-(2,5-dimethylphenyl)-1H-1,2,4-triazol-5(4H)-one (**11r**)

1H NMR (300 MHz, $CDCl_3$, TMS): δ 8.15 (s, 1H), 7.78 (s, 1H), 7.41 (s, 1H), 6.78–7.55 (m, 6H), 5.30 (s, 1H), 4.51 (s, 2H), 3.88 (t, $J = 6.9$ Hz, 2H), 3.07 (d, $J = 13.5$ Hz, 1H), 2.66 (d, $J = 13.5$ Hz, 1H), 2.36 (br, 10H), 2.34 (s, 3H), 2.19 (s, 3H), 1.94 (m, 2H). MS (ESI) m/z : 553 ($M + 1$). Anal. calcd for $C_{28}H_{34}F_2N_8O_2$: C 60.86, H 6.20, N 20.28, found: C 60.92, H 6.21, N 20.21.

6.1.24. 1-(3-(4-(2-(2,4-Difluorophenyl)-2-hydroxy-3-(1H-1,2,4-triazol-1-yl)propyl) piperazin-1-yl)propyl)-4-(2,6-dimethylphenyl)-1H-1,2,4-triazol-5(4H)-one (**11s**)

1H NMR (300 MHz, $CDCl_3$, TMS): δ 8.14 (s, 1H), 7.79 (s, 1H), 7.34 (s, 1H), 6.78–7.55 (m, 6H), 5.31 (s, 1H), 4.51 (s, 2H), 3.90 (t, $J = 7.0$ Hz, 2H), 3.07 (d, $J = 13.5$ Hz, 1H), 2.66 (d, $J = 13.5$ Hz, 1H), 2.36 (br, 10H), 2.16 (s, 6H), 1.94 (m, 2H). MS (ESI) m/z : 551 ($M - 1$). Anal. calcd for $C_{28}H_{34}F_2N_8O_2$: C 60.86, H 6.20, N 20.28, found: C 60.80, H 6.21, N 20.26.

6.1.25. 1-(3-(4-(2-(2,4-Difluorophenyl)-2-hydroxy-3-(1H-1,2,4-triazol-1-yl)propyl) piperazin-1-yl)propyl)-4-(4-methyl-3-nitrophenyl)-1H-1,2,4-triazol-5(4H)-one (**11t**)

1H NMR (500 MHz, $CDCl_3$, TMS): δ 8.13 (s, 1H), 7.78 (s, 1H), 6.78–8.20 (m, 6H), 7.78 (s, 1H), 5.30 (br, 1H), 4.50 (d, $J_1 = 4.3$ Hz,

2H), 3.88 (t, $J = 6.9$ Hz, 2H), 3.04 (d, $J = 13.6$ Hz, 1H), 2.63 (d, $J = 13.5$ Hz, 1H), 2.64 (s, 3H), 2.35 (br, 10H), 1.92 (m, 2H). Anal. calcd for $C_{27}H_{31}F_2N_9O_4$: C 55.57, H 5.35, N 21.60, found: C 55.40, H 5.37, N 21.64.

6.2. Flexible docking analysis

The 3D structure of CACYP51 was built by homology modeling [9]. Flexible ligand docking procedure in the Affinity module within InsightII software package was used to define the lowest energy position for the compound **11c** using a Monte Carlo docking protocol. The detailed docking parameters were from our previous studies [11].

Acknowledgment

This work was supported by the National Natural Science Foundation of China (Grant No. 30930107), Shanghai Rising-Star Program (Grant No. 09QA1407000) and Shanghai Leading Academic Discipline Project (Project No. B906).

References

- [1] J.J. Caston-Osorio, A. Rivero, J. Torre-Cisneros, Int. J. Antimicrob. Agents 32 (Suppl. 2) (2008) S103–S109.
- [2] M. Cuenca-Estrella, L. Bernal-Martinez, M.J. Buitrago, M.V. Castelli, A. Gomez-Lopez, O. Zaragoza, J.L. Rodriguez-Tudela, Int. J. Antimicrob. Agents 32 (Suppl. 2) (2008) S143–S147.
- [3] L. Ostrosky-Zeichner, K.A. Marr, J.H. Rex, S.H. Cohen, Clin. Infect. Dis. 37 (2003) 415–425.
- [4] G. Aperis, E. Mylonakis, Expert Opin. Investig. Drugs 15 (2006) 579–602.
- [5] C.A. Kauffman, P.L. Carver, Semin. Respir. Crit. Care Med. 29 (2008) 211–219.
- [6] Y. Aoyama, Y. Yoshida, R. Sato, J. Biol. Chem. 259 (1984) 1661–1666.
- [7] H. Ji, W. Zhang, Y. Zhou, M. Zhang, J. Zhu, Y. Song, J. Lu, J. Med. Chem. 43 (2000) 2493–2505.
- [8] C. Sheng, Z. Miao, H. Ji, J. Yao, W. Wang, X. Che, G. Dong, J. Lu, W. Guo, W. Zhang, Antimicrob. Agents Chemother. 53 (2009) 3487–3495.
- [9] C. Sheng, W. Wang, X. Che, G. Dong, S. Wang, H. Ji, Z. Miao, J. Yao, W. Zhang, ChemMedChem 5 (2010) 390–397.
- [10] C. Sheng, W. Zhang, M. Zhang, Y. Song, H. Ji, J. Zhu, J. Yao, J. Yu, S. Yang, Y. Zhou, J. Lu, J. Biomol. Struct. Dyn. 22 (2004) 91–99.
- [11] C. Sheng, W. Zhang, H. Ji, M. Zhang, Y. Song, H. Xu, J. Zhu, Z. Miao, Q. Jiang, J. Yao, Y. Zhou, J. Lu, J. Med. Chem. 49 (2006) 2512–2525.
- [12] X. Che, C. Sheng, W. Wang, Y. Cao, Y. Xu, H. Ji, G. Dong, Z. Miao, J. Yao, W. Zhang, Eur. J. Med. Chem. 44 (2009) 4218–4226.
- [13] W. Wang, C. Sheng, X. Che, H. Ji, Y. Cao, Z. Miao, J. Yao, W. Zhang, Bioorg. Med. Chem. Lett. 19 (2009) 5965–5969.
- [14] W. Wang, C. Sheng, X. Che, H. Ji, Z. Miao, J. Yao, W.N. Zhang, Arch. Pharm. (Weinheim) 342 (2009) 732–739.
- [15] Y. Xu, C. Sheng, W. Wang, X. Che, Y. Cao, G. Dong, S. Wang, H. Ji, Z. Miao, J. Yao, W. Zhang, Bioorg. Med. Chem. Lett. 20 (2010) 2942–2945.
- [16] T. Cheng, Y. Zhao, X. Li, F. Lin, Y. Xu, X. Zhang, Y. Li, R. Wang, L. Lai, J. Chem. Inf. Model. 47 (2007) 2140–2148.
- [17] N. Isham, M.A. Ghannoum, J. Clin. Microbiol. 44 (2006) 4342–4344.
- [18] H. Ji, W. Zhang, M. Zhang, M. Kudo, Y. Aoyama, Y. Yoshida, C. Sheng, Y. Song, S. Yang, Y. Zhou, J. Lu, J. Zhu, J. Med. Chem. 46 (2003) 474–485.
- [19] L.M. Lima, E.J. Barreiro, Curr. Med. Chem. 12 (2005) 23–49.
- [20] G.A. Patani, E.J. LaVoie, Chem. Rev. 96 (1996) 3147–3176.